

Fig. S1 (a) XRD patterns of LLZTO-air and LLZTO-HT powders; (b) SEM image of LLZTO-air powders; (c) TEM; (d)HRTEM image of LLZTO-air powders; (e) SEM image of LLZTO-HT powders; (f) TEM; (g)HRTEM image of LLZTO-HT powders.

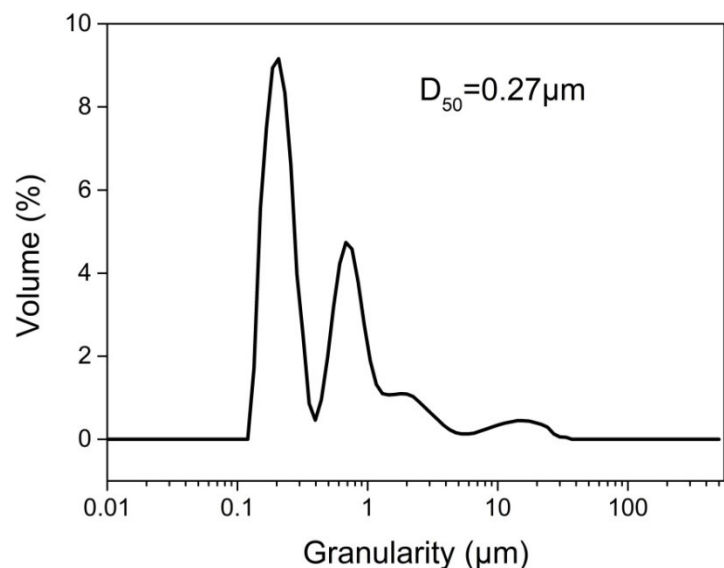


Fig. S2 Particle size distributions of LLZTO-HT powders.

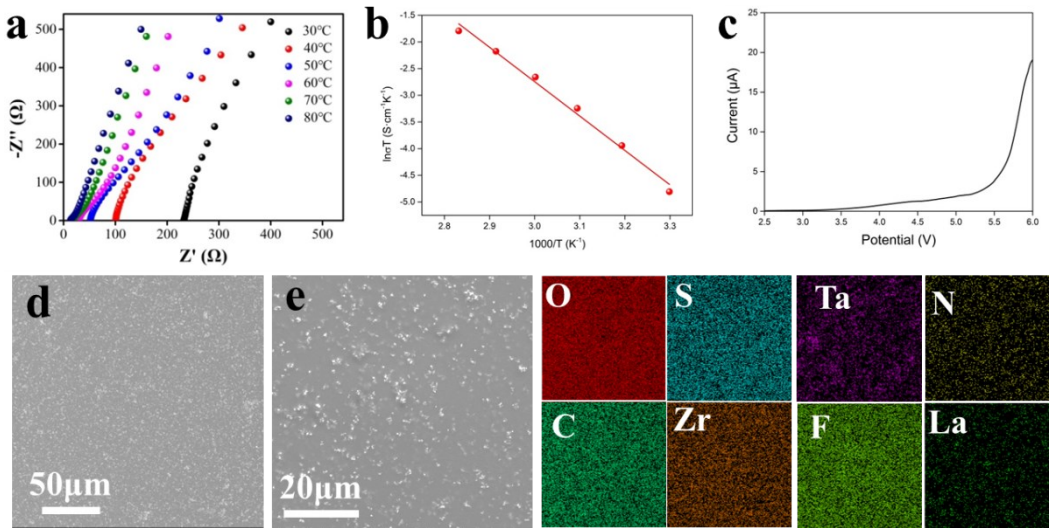


Fig. S3 (a) AC impedance spectra of PLEs in the temperature range from 30 to 80°C; (b) Arrhenius plots for the ionic conductivity in the temperature range from 30 to 80°C; (c) LSV curve of PLEs; (d) SEM of PLEs; (e) SEM and EDS elemental mapping of O, S, Ta, N, C, Zr, F and La for PLEs.

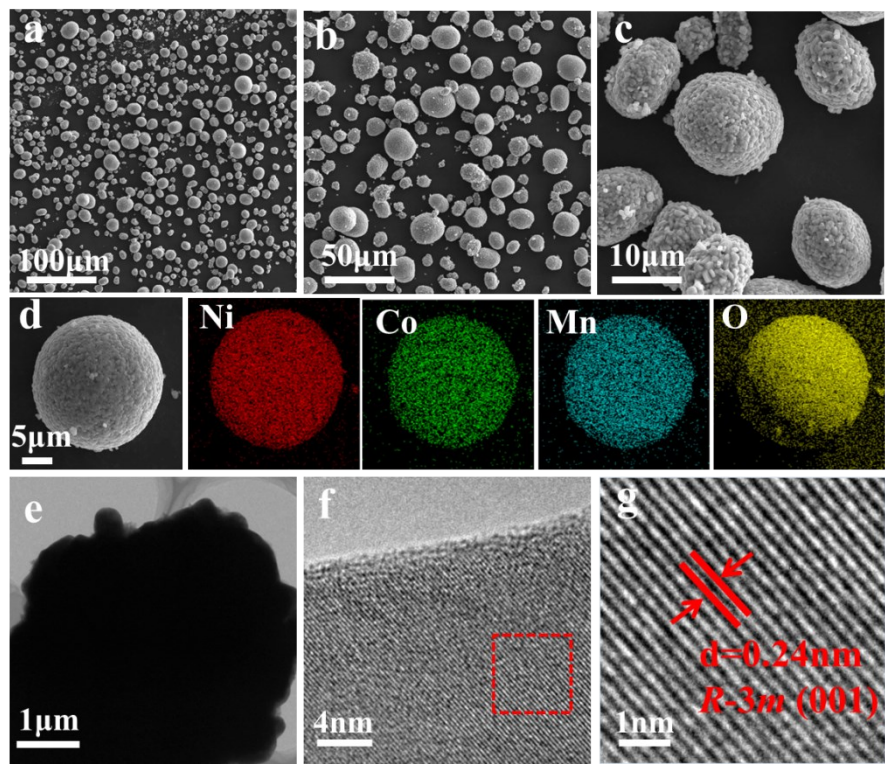


Fig. S4 Morphology and elemental distribution of PC-NCM613. (a, b, c)SEM images of PC-NCM613 powders; (d) EDS elemental mapping of Ni, Co, Mn, O for PC-NCM particle; (e)TEM; (f, g)HRTEM images.

Table S1. Rietveld refinement results of the PC-NCM sample.

Formula		PC-NCM			
Space group		R-3m			
		x	y	z	g
Li1	3b	0	0	1/2	0.9768
Ni2	3b	0	0	1/2	0.0232
Li2	3a	0	0	0	0.0232
Mn	3a	0	0	0	0.3
Co	3a	0	0	0	0.1
Ni1	3a	0	0	0	0.5768
O	6c	0	0		1
a-axis/Å				2.874(2)	
c-axis/Å				14.235(0)	
Volume /Å³				101.838	
R _{wp} /%				3.37	
R _p /%				2.37	

Table S2. Rietveld refinement results of the SC-NCM sample

Formula		SC-NCM			
Space group		R-3m			
		x	y	z	g
Li1	3b	0	0	1/2	0.9894
Ni2	3b	0	0	1/2	0.0106
Li2	3a	0	0	0	0.0106
Mn	3a	0	0	0	0.3
Co	3a	0	0	0	0.1
Ni1	3a	0	0	0	0.5894
O	6c	0	0		1
a-axis /Å				2.893(1)	
c-axis /Å				14.325(5)	
Volume /Å³				103.841	
R _{wp} /%				3.84	
R _p /%				2.68	

Table S3 Chemical compositions of Ni, Co, and Mn for the PC-NCM and SC-NCM powders measured by ICP-OES test.

Sample	Chemical composition (at. %)		
	Ni	Co	Mn
PC-NCM613	60.7	9.2	30.1
SC-NCM613	60.1	10.1	29.8

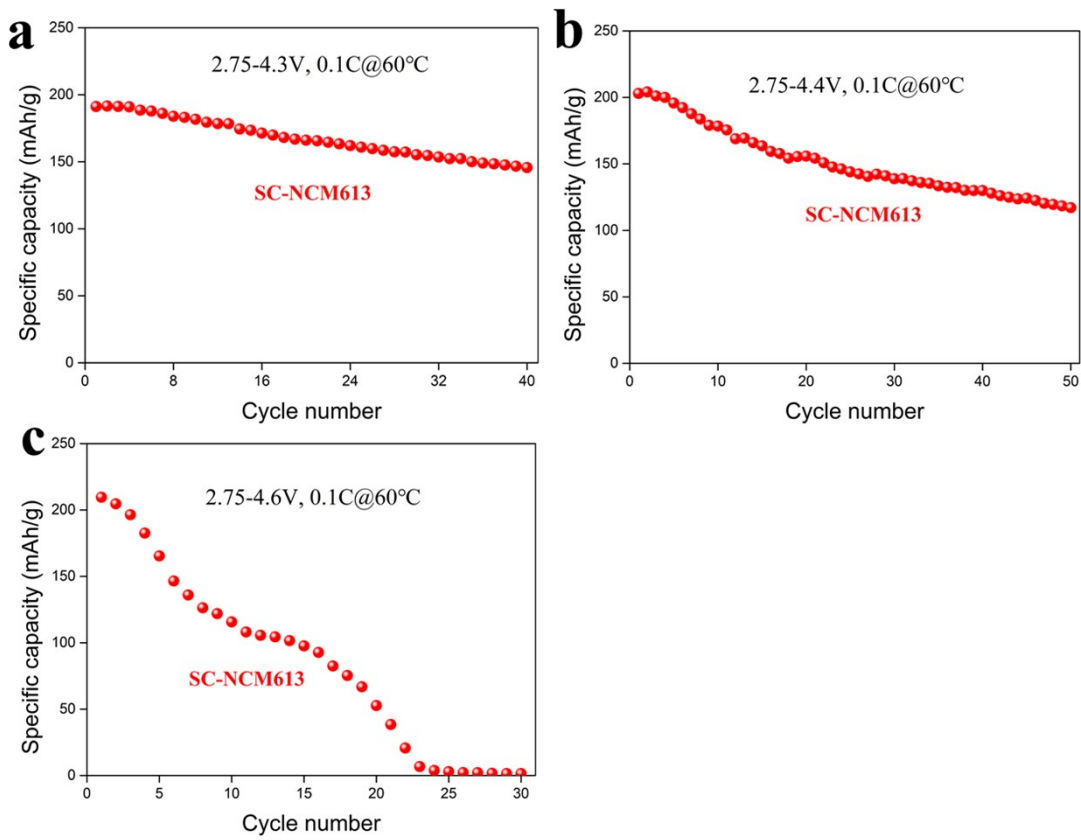


Fig. S5 (a) Cycling performance of SC-NMC613 with the voltage range of 2.75-4.3 V at 0.1C; (b) cycling performance of SC-NMC613 with the voltage range of 2.75-4.4 V at 0.1C; (c) cycling performance of SC-NMC613 with the voltage range of 2.75-4.6 V at 0.1C

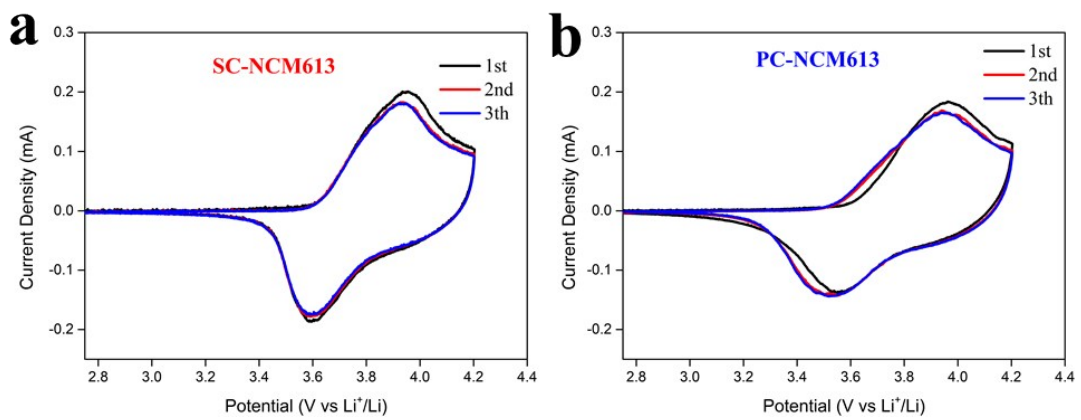


Fig. S6 (a) CV of initial three cycles of SC-NCM613; (b) CV of initial three cycles of PC-NCM613.

Table S4 Summary of performance of NCM cathodes in ASSBs with PEO-based electrolytes reported in literatures and this work.

year	Composition	Active Materials	Potential range	initial capacity (mAh/g)	Cycle performance	Ref.
2019	PEG+LiTFSI+LiBOB	PC-NCM111	2.8-4.2V	130.1(1/3C)	26.3 (1/3C, 40cycles)	1
			2.8-4.25V	135 (1/3C)	19.3 (1/3C, 40cycles)	
2019	PEO+LiClO ₄ +Al-LLZO	PC-NCM424	3.0-4.1V	122(0.1C, 70°C)	97.6(0.1C, 100cycles, 70°C)	2
2020	PEO+LiTFSI	PC-NCM622	3-4.2V	153(0.2C, 60°C)	76.5(0.2C, 100cycles, 60°C)	3
2020	PEO+LiClO ₄ +LLZTO	PC-NCM811	2.8-4.3V	204.8(0.1C, 60°C)	73.9(0.2C, 50cycles, 60°C)	4
2020	PEO/EC/LiClO ₄ /LLZTO	PC-NCM811	2.8-4.3V	167(0.1C, 60°C)		5
2020	PEO+LiTFSI+LiClO ₄ +Al-LLOZO	PC-NCM622	3-4.1V	169(0.1C, 70°C)		6
				158(1/3C,70°C)	126(1/3C, 100cycles, 70°C)	
2020	PEO+LiClO ₄ +Al-LLZO+Ga-LLZO	PC-NCM424	3-4.1V	131(0.1C, 70°C)		7
				100(1/3C,70°C)	93(1/3C, 100cycles, 70°C)	
2020	PEG+LiTFSI+LiFSI	PC-NCM523	2.5-4.3V	130(0.2C, 60°C)	19(0.2C, 100cycles, 60°C)	8
2020	PEO+LiTFSI+LiBOB+LiPF ₆ +PEGDME+EC/PC	PC-NCM523	3-4.3V	150(0.3C, 60°C)	58.8(0.3C, 50cycles, 60°C)	9
this work	PEO+LiTFSI+LLZTO	PC/SC-NCM613	2.75-4.2V	166/167(0.1C, 60°C)		
				149.7/156.8(0.2C, 60°C)		
				137.5/152.1(0.5C, 60°C)	90.1/108.8(0.5C, 100cycles, 60°C)	
				120.1/147.8(1C, 60°C)	61.2/90.4(1C, 100cycles, 60°C)	
				117.5/143.2(3C, 60°C)	33.2/90.8(3C, 50cycles, 60°C)	
		SC-NCM613	2.75-4.3V	191.2(0.1C, 60°C)	145.7(0.1C, 40cycles, 60°C)	

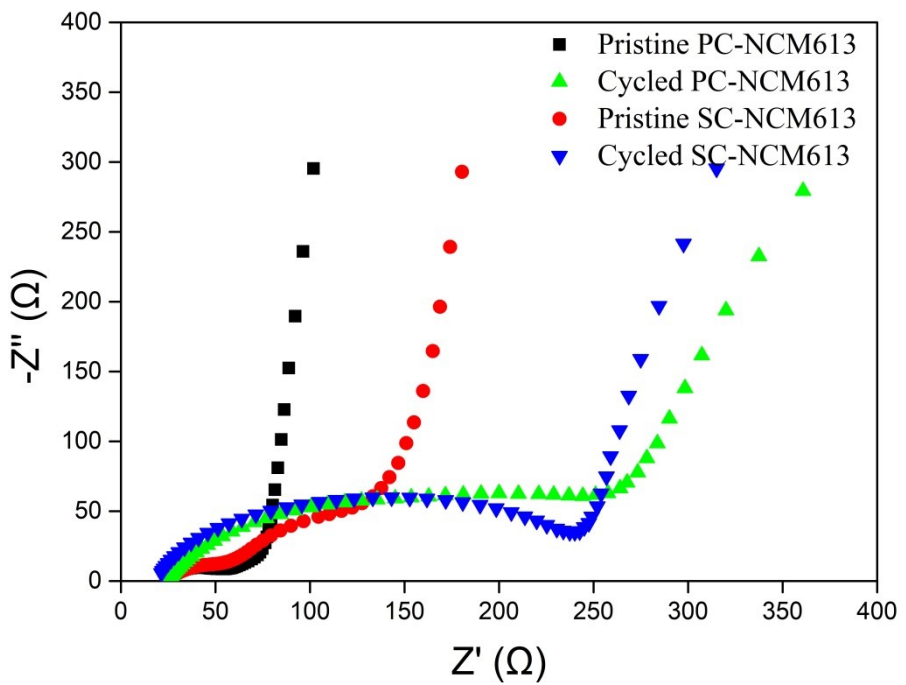


Fig. S7 EIS results of pristine and cycled NCM613.

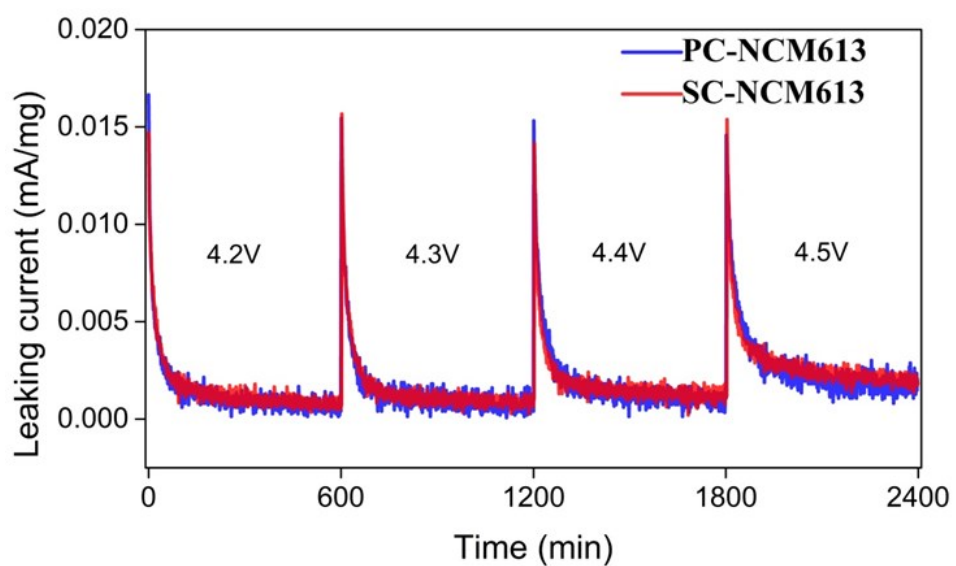


Fig. S8 Leakage current density of SC-NCM613 and PC-NCM613.

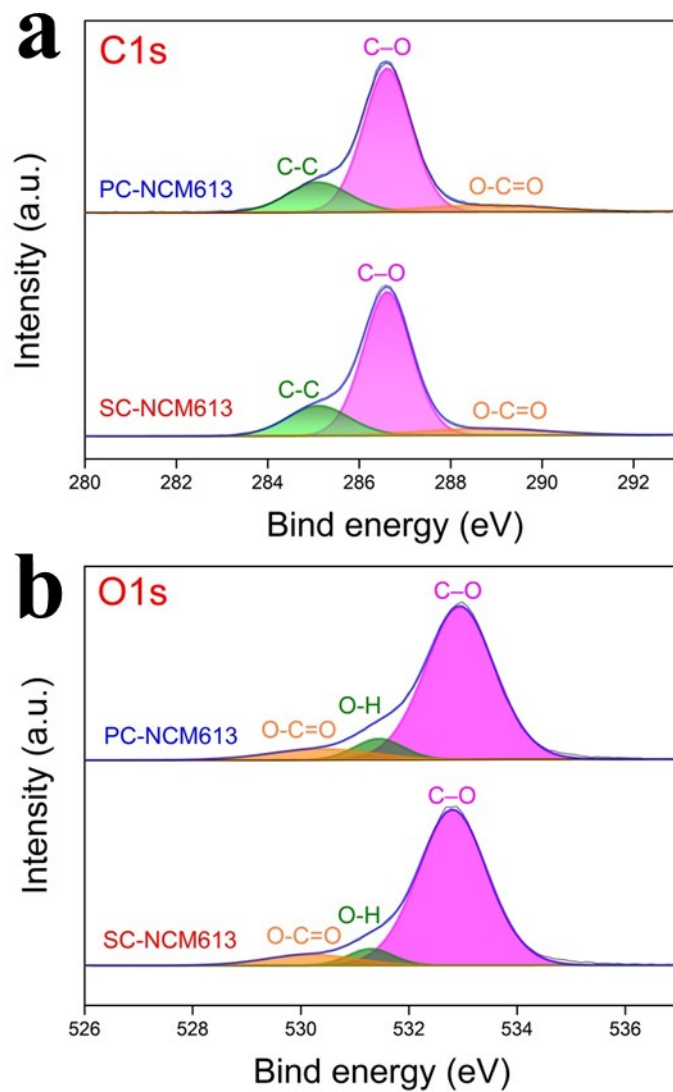


Fig S9 (a) C1s XPS spectra of NMC613 electrode; (b) O1s XPS spectra of NMC613 electrode.

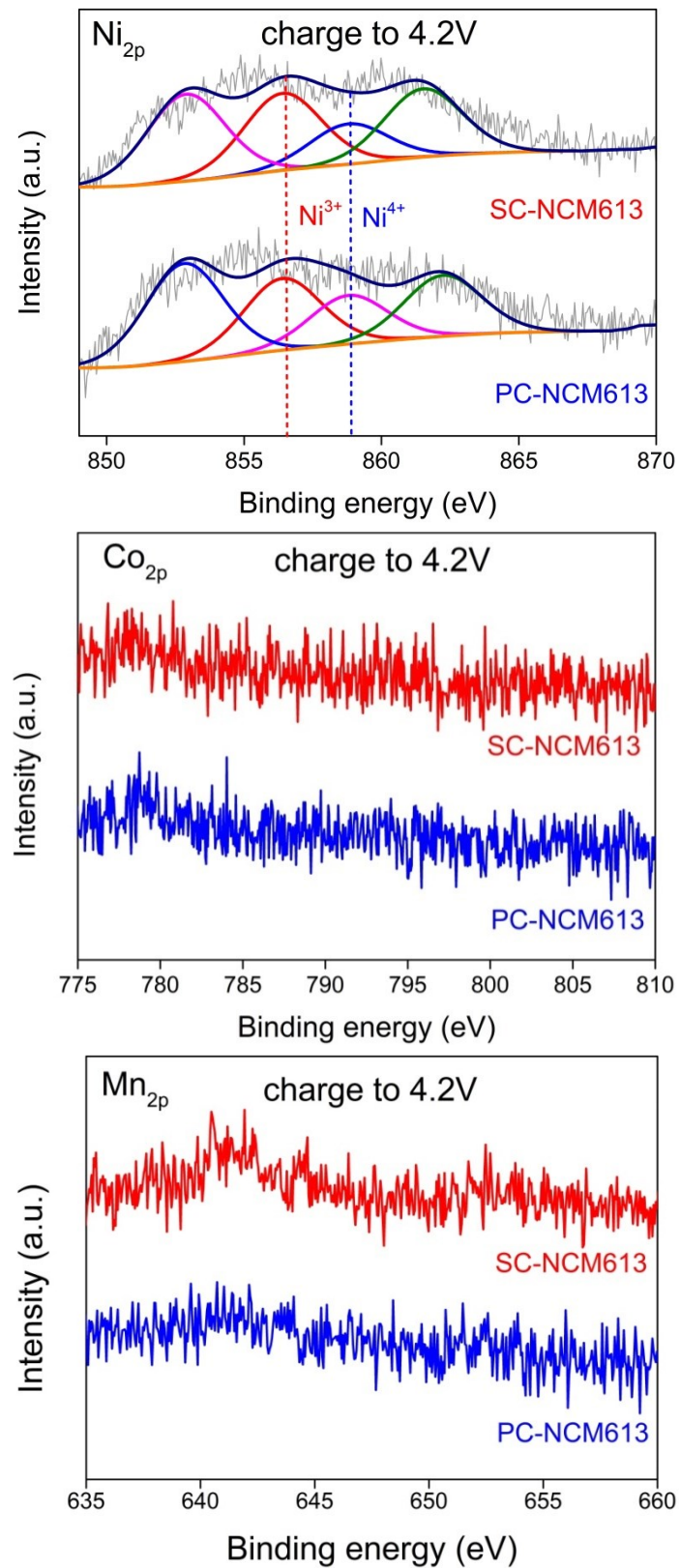


Fig. S10 XPS Ni 2p, Co 2p and Mn 2p spectra of the cathode surface for charged to 4.2V at 1C.

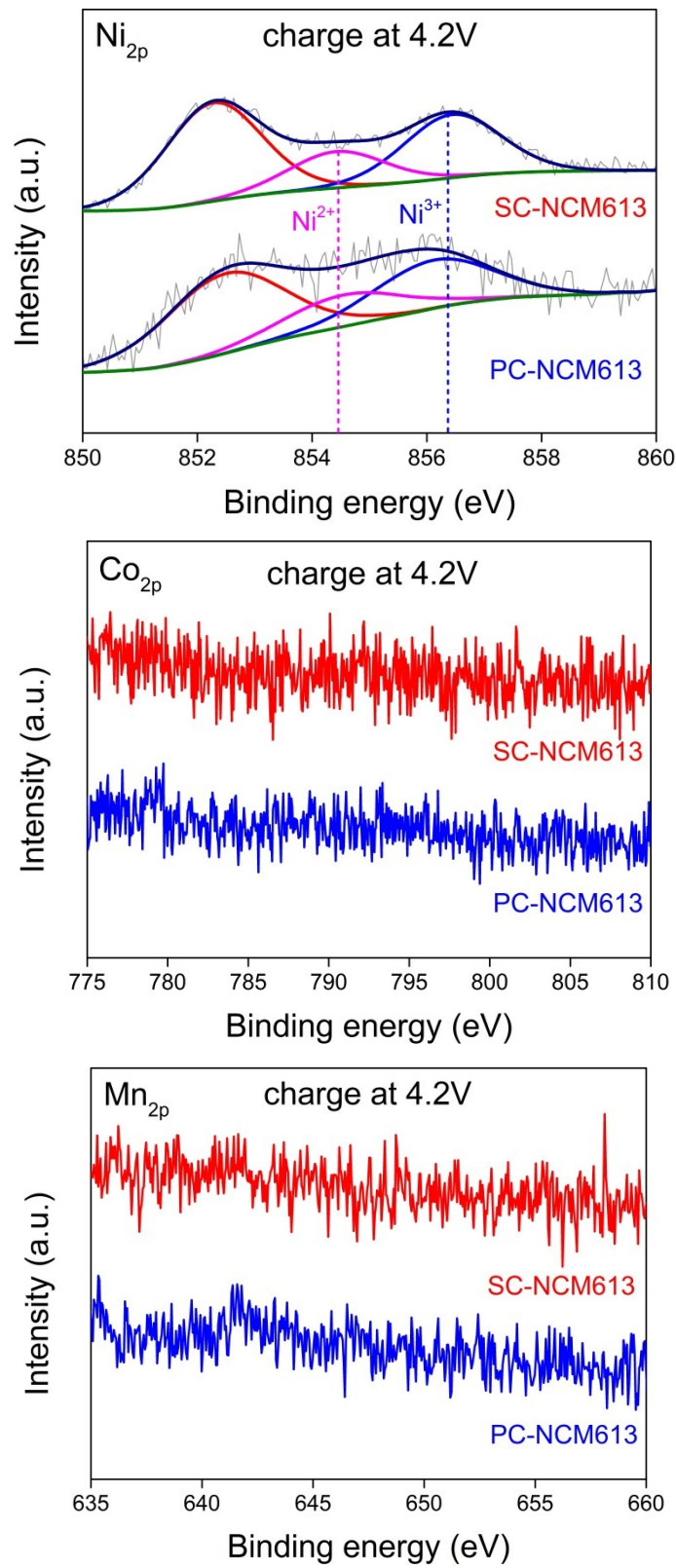


Fig. S11 XPS Ni 2p, Co 2p and Mn 2p spectra of the cathode surface for charged at 4.2V until the current is less than 0.1C .

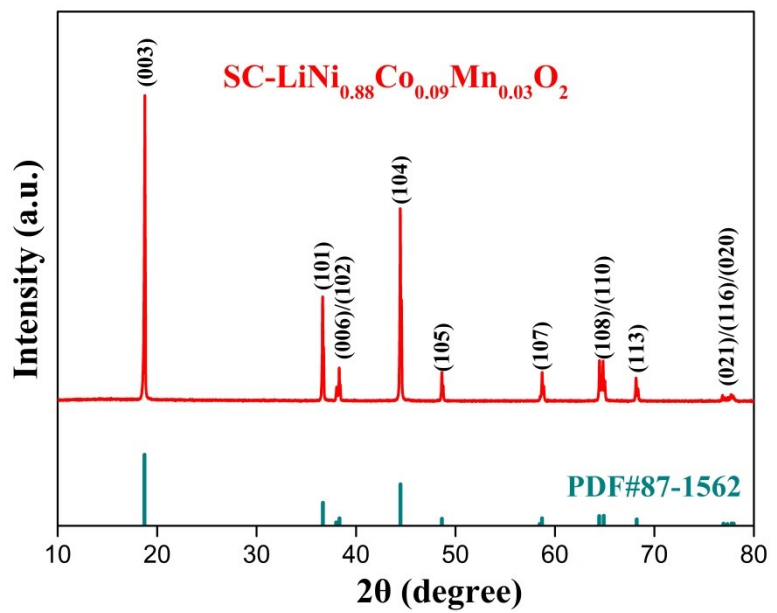


Fig. S12 XRD pattern of SC-LiNi_{0.88}Co_{0.09}Mn_{0.03}O₂ powders.

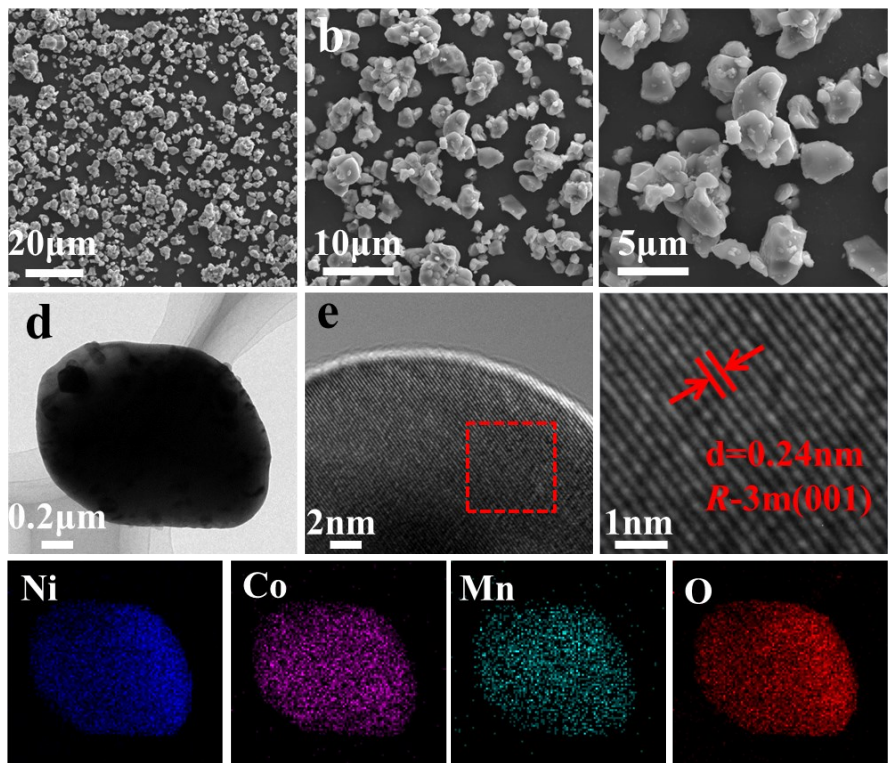


Fig. S13 Morphology and elemental distribution of SC-LiNi_{0.88}Co_{0.09}Mn_{0.03}O₂. (a, b, c)SEM images of SC-LiNi_{0.88}Co_{0.09}Mn_{0.03}O₂ powders; (d)TEM and EDS elemental mapping of Ni, Co, Mn, O for SC-LiNi_{0.88}Co_{0.09}Mn_{0.03}O₂ particle; (e)HRTEM image.

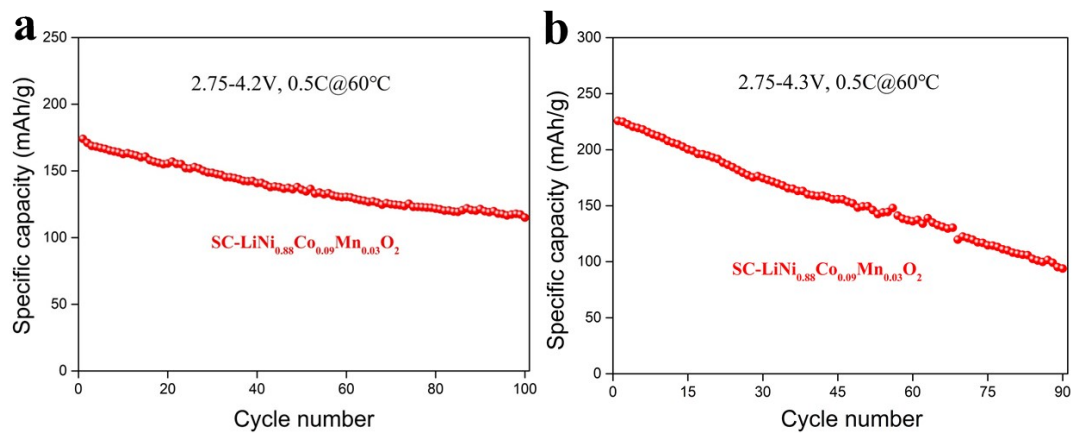


Fig. S14 (a) Cycling performance of SC-LiNi_{0.88}Co_{0.09}Mn_{0.03}O₂ with the voltage range of 2.75-4.2 V at 0.5C; (b) cycling performance of SC-LiNi_{0.88}Co_{0.09}Mn_{0.03}O₂ with the voltage range of 2.75-4.3 V at 0.5C.

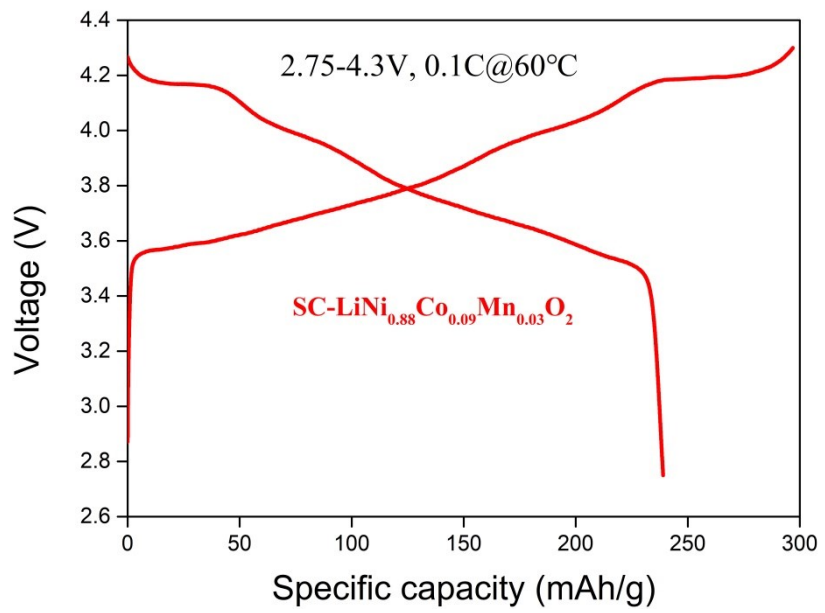


Fig. S15 The initial charging-discharging curves at 0.1C with the voltage range of 2.75-4.3 V of SC-LiNi_{0.88}Co_{0.09}Mn_{0.03}O₂ at 60 °C

References

- [S1] H. Zhai, T. Gang, B. Xu, Q. Cheng, D. Paley, B. Qie, T. Jin, Z. Fu, L. Tan, Y.H. Lin, C.W. Nan, Y. Yang, ACS Appl. Mater. Interfaces, 2019, 11, 28774.
- [S2] D.H. Kim, M.Y. Kim, S.H. Yang, H.M. Ryu, H.Y. Jung, H.J. Ban, S.J. Park, J.S. Lim, H.S. Kim, J. Ind. Eng. Chem., 2019, 71, 445.
- [S3] J. Tan, X. Ao, H. Zhuo, L. Zhuang, X. Huang, C. Su, W. Tang, X. Peng, B. Tian, , Chem. Eng.J., 2020, 127623.
- [S4] J. Liang, S. Hwang, S. Li, J. Luo, Y. Sun, Y. Zhao, Q. Sun, W. Li, M. Li, M.N. Banis, X. Li, R. Li, L. Zhang, S. Zhao, S. Lu, H. Huang, D. Su, X. Sun, Nano Energy, 2020, 78, 105107.
- [S5] S.H.S. Cheng, C. Liu, F. Zhu, L. Zhao, R. Fan, C.Y. Chung, J. Tang, X. Zeng, Y.B. He, Nano Energy, 2021, 80, 105562.
- [S6] S.J. Park, M.Y. Kim, J.S. Lim, B.-S. Kang, Y.A. Kim, Y.S. Hong, H.C. Kim, H.S. Kim, J. Electrochem. Soc., 2020, 167, 090551.
- [S7] H.Y. Jung, M.Y. Kim, S.H. Yang, S.J. Park, H.M. Ryu, H.J. Ban, J.H. Han, H.S. Kim, Ionics, 2020, 26, 4783.
- [S8] X. Yang, M. Jiang, X. Gao, D. Bao, Q. Sun, N. Holmes, H. Duan, S. Mukherjee, K. Adair, C. Zhao, J. Liang, W. Li, J. Li, Y. Liu, H. Huang, L. Zhang, S. Lu, Q. Lu, R. Li, C.V. Singh, X. Sun, Energy Environ. Sci., 2020, 13, 1318.
- [S9] Z. Li, A. Li, H. Zhang, R. Lin, T. Jin, Q. Cheng, X. Xiao, W.K. Lee, M. Ge, H. Zhang, A. Zangiabadi, I. Waluyo, A. Hunt, H. Zhai, J.J. Borovilas, P. Wang, X.Q. Yang, X. Chuan, Y. Yang, Nano Energy, 2020, 72, 104655.